KMITL Sci. Tech. J. Vol. 7 No. 2 Jul. - Dec. 2007

A STATISTICAL CHARACTERIZATION FOR POROUS MEDIA STRUCTURES

Phongsan Meekunnasombat[1*] and Florian Fichot[2]

[1]Department of Mechanical Engineering, Faculty of Engineering
Naresuan University, Phitsanulok 65000, Thailand
[2]Institut de Radioprotection et de Sûreté Nuclèaire (IRSN)
DPAM/SEMCA/LESAG - Bât.700 BP3, 13115 St-Paul-lez-Durance, France

ABSTRACT

Some porous media structures may appear complicated at first glance. With proper treatments, these structures may be simplified and characterized for further analysis. In this paper, a method to statistically characterize the structure of a porous media is presented. Tomography images of a severely damaged nuclear reactor core are used as samples to develop the proposed method. It is found that the particle and void size distributions of the samples can be obtained. These distributions appear to be good representations of the damage degree of the corresponding locations. They may be fitted by the sum of standard beta distribution functions which are easier to use for a physical and mathematical modeling of such porous structure. It is expected that this method can also be applied to different types of porous structure in other applications.

KEYWORDS: porous media, distribution function, curve fitting, tomography, reactor core, severe accident

1. INTRODUCTION

Porous media play a vital role in many engineering applications, such as, studies of soil structure for agricultural and petroleum applications, studies of shock-absorption materials [1], studies of fluid flow in complex porous structure [2], and many more. Characterizing the physical structure of these materials has always been a challenge. A method to statistically characterize the porous structure presented in this paper has been developed as a support to IRSN safety studies [3-4]. The medium used here is of a severely damaged nuclear fuel bundle from PHEBUS experiments [5].

In case of a severe accident in a Pressurized Water Reactor (PWR), fuel assemblies are likely to be significantly damaged, broken or even melted. The geometry of the core evolves from an essentially 1D anisotropic configuration to a much more isotropic configuration favoring the existence of multidimensional flows. Figure 1 shows an example of tomography density field reconstruction of the core before and after being damaged from neutronic heating in PHEBUS experiments.

*Corresponding author: Tel: +66 (0)55-261000 ext 4179
E-mail: phongsan@gmail.com

To investigate the coolability of this material, it is necessary to know accurately some characteristic geometrical parameters such as the mean distance between two damaged rods, the size of rods or particles, surface area between the particles and the fluids, etc. These parameters can be obtained by means of the characterization method presented in this paper. First, the image is simplified with appropriate density thresholds then scanned to obtain its solid and void size distributions. Although the structure of the material is seen complicated, its size distribution is not. These size distributions are then characterized with mathematical expressions where only a few numerical parameters are introduced.

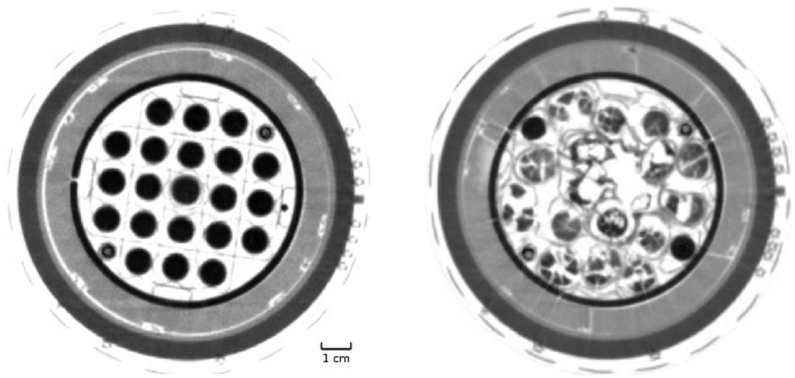

(a) Initial core (b) Damaged core

Figure 1 Tomography density field reconstructions (at the middle of the test bundle) from a PHEBUS experiment.

2. ACQUIRING DISTRIBUTION

The method of acquiring data from the tomograph of the medium may be divided in two steps. First, a tomography density field reconstruction (such as shown in Figure 1) is transformed into a binary image where the interfaces between void and particles are clearly visible, without taking the bundle enclosure into account, as shown in Figure 2. Since the density resolution of the tomography process is approximately 2 g/cc, any material seen less than that is considered as void (the white areas in Figure 2a). For particles, it is chosen any material with density greater than 6 g/cc to be non-accessible for the coolant (the black areas in Figure 2b). The reading between 2 to 6 g/cc is considered as an uncertainty of the measurement.

In the second step, a scan of the image is made to determine the chord-length of the impermeable part (*i.e.*, particle), when detecting the areas with density > 6 g/cc, or void, when detecting the areas with density < 2 g/cc, distribution such as shown in Figure 3 The pixel-by-pixel scan is made in the two main perpendicular directions of the image. Obviously, scanning along those two preferential directions induces a statistical bias for asymmetric particles. However, as this is a first exploratory study, we did not try to improve the accuracy of the image analysis algorithm. Nevertheless, we have shown that this algorithm allows to characterize the initial, non-damaged, geometry (such as shown in Figure 1a) with a sufficient accuracy (average particle size of 8 mm is identified by the highest peak in Figure 4, and average void size of 2 mm), which shows that the vertical and horizontal distribution of chord-length provides a reasonable representation of the particle and void size.

(a) < 2 g/cc for voids (white areas)

(b) > 6 g/cc for particles (black areas)

Figure 2 Binary images of Figure 1b at two different density thresholds.

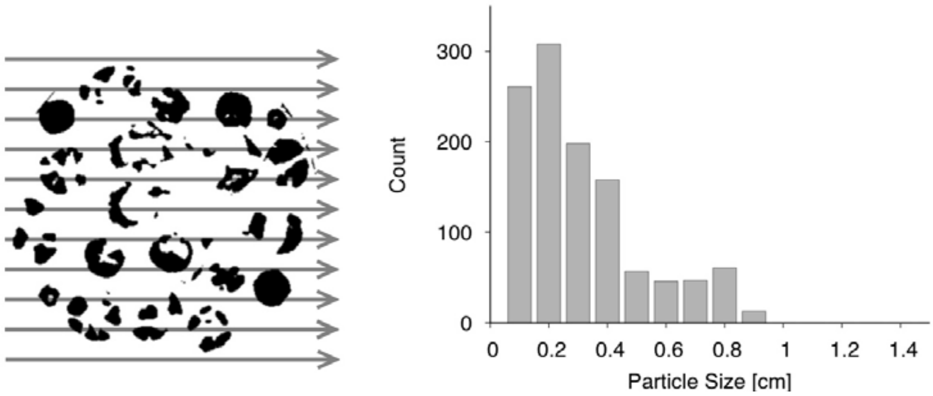

(a) Filtered tomography (> 6 g/cc) and scanning line of sight

(b) Chord-length distribution

Figure 3 A tomography reconstruction of density field (from Figure 2b) is filtered and scanned across (a) to generate a chord-length distribution (b).

3. DISTRIBUTION FUNCTION

In order to fit the obtained distributions, it was assumed that they resulted from the sum of two functions. The first function would represent the particles remaining from the initial state and the second one would represent the particles obtained after degradation (fragmentation or melting). The beta distribution function is an excellent candidate because it is defined over a finite range and flexible enough, with two positive shape parameters, α and β, to be conveniently adjusted to many shapes. The size distributions (*e.g.*, Figure 3b) appear to compose of two distinct shapes of different features, hence the complete fitting function is essentially a summation of two basic distribution functions. A general form of the beta distribution function is [6],

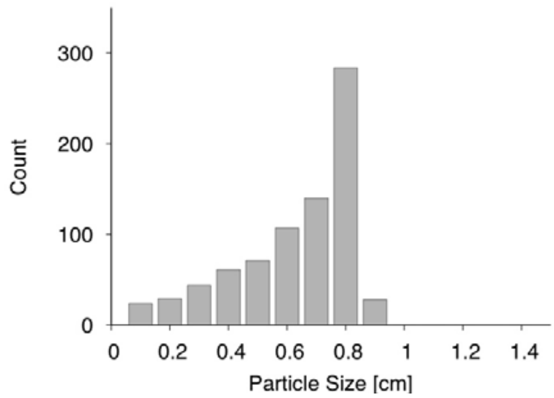

Figure 4 Chord-length distribution of a non-damaged section (Figure 1a).

$$f(x) = \frac{x^{\alpha-1}(1-x)^{\beta-1}}{\mathbf{B}(\alpha,\beta)} \tag{1}$$

where x is the member, which represents the particle/void size in this case, with the range of [0,1] and $\int_0^1 f(x)dx = 1$. The definition of the beta function is,

$$\mathbf{B}(\alpha,\beta) = \int_0^1 x^{\alpha-1}(1-x)^{\beta-1}dx \tag{2}$$

$$= \frac{\Gamma(\alpha)\Gamma(\beta)}{\Gamma(\alpha+\beta)}. \tag{3}$$

The particle and void size, ℓ_p and ℓ_v, which have a range of $[\ell_{\min}, \ell_{\max}]$, must be normalized to x = [0,1] with factor $\eta = N/n_{\text{bin}}$, where N is the total number of member and n_{bin} is the number of "bin" in the acquired distribution. Then the shape parameters are estimated with,

$$\hat{\alpha} = \bar{x}\left\{\left(\frac{\bar{x}(1-\bar{x})}{\sigma^2}\right) - 1\right\} \tag{4}$$

$$\hat{\beta} = (1-\bar{x})\left\{\left(\frac{\bar{x}(1-\bar{x})}{\sigma^2}\right) - 1\right\} \tag{5}$$

Where $\bar{x}$ is the mean value of the normalized members, $\frac{1}{N}\sum_{i=1}^{N} x_i$, and σ^2 is the variance, $\frac{1}{N}\sum_{i=1}^{N}(x_i - \bar{x})^2$. The initial distribution function, *f(x)*, is calculated. A least-squares optimization is then applied to adjust the shape parameters to minimize the error to the acquired data. Finally, before the optimized distribution function can be compared with the input data, it must be reverted by η, the same factor that normalized ℓ_p and ℓ_v.

The scanned size distribution is divided into two parts to determine the two beta functions separately as described above, then combined to form a complete distribution function. Therefore, each size distribution can be described with the total of 4 shape parameters; α_1, β_1, and α_2, β_2. Hence, the complete distribution function is

$$g(\ell) = \eta_1 f_1(x, \alpha_1, \beta_1) + \eta_2 f_2(x, \alpha_2, \beta_2). \tag{6}$$

The detailed procedure of how the input distribution is separated and fit with the distribution function is described in the next section.

4. FITTING PROCEDURE

As mentioned in the previous section, the size distributions appear to compose of two distinct parts. Therefore, it is necessary to separate these parts and fit individually with the distribution function. The input distribution shown in Figure 3b is used as a numerical example. The fitting procedure is the following:

i) The maximum size in the distribution is identified to set the upper limit of the distribution function (it is 1 cm in the case of Figure 3b). This upper limit, ψ, will be used to normalize the data.

ii) The first lowest point or "valley" is identified (0.6 cm in the example) then a straight line is drawn from this point to ψ. This line divides the distribution into two parts.

iii) The data on the left of (and below) the separation line is the first set to be fit with the distribution function.

iv) Normalize the data from ℓ_p or ℓ_v to *x* with,

$$x = \frac{\ell - \ell_{\min}}{\psi - \ell_{\min}}. \tag{7}$$

v) Estimate the shape parameters, $\hat{\alpha}$ and $\hat{\beta}$, from Eqns. (4) and (5).

vi) Use the standard least-squares method to minimize the error between the data and the initial distribution function to get the optimized shape parameters, α and β.

vii) Calculate the scaling parameter, η (in Section 3), in which the newly determined distribution function in the physical domain, $g_1(\ell)$, is $\eta_1 f_1(x)$.

viii) Subtract the original data with the first set of data for the second set (the data on the right of (and above) the separation line drawn in step *ii*). Then repeat step *iv* thru *vii* for the second distribution function, $g_2(\ell)$.

ix) Derive the total distribution function, $g(\ell)$, by simply summing the two functions as shown in Eqn. (6).

5. SAMPLE RESULTS

Examples of the particle size distribution obtained from degraded sections of the test bundle (FPT1) are shown in Figure 5. One can see that the distribution shifts toward the left (the smaller sizes) when the section appears to be more fragmented (the binary images on the upper-right corner of the distributions). The approximate distribution functions are shown by the dotted lines over the bar graphs. It is seen that these functions match well with the acquired data, which provides an indication of the state of degradation of the porous structure. As a result, the size distribution can be represented with 4 shape parameters of the distribution function, namely; α_1, β_1, and α_2, β_2.
Interestingly, from Eqns. (4) and (5), the ratio of the estimated shape parameters is,

$$\frac{\hat{\beta}}{\hat{\alpha}} = \frac{(1-\bar{x})}{\bar{x}}. \tag{8}$$

It is found that this relationship is still valid for both particle and void size even after the least-squares optimization with only an additional constant being introduced,

$$\left(\frac{\beta_1}{\alpha_1}\right)_{p,v}, \left(\frac{\beta_2}{\alpha_2}\right)_{p,v} \propto \frac{\left(1-\bar{x}_{p,v}\right)}{\bar{x}_{p,v}}. \tag{9}$$

Hence, knowing *either* α or β, the other can be explicitly determined from the knowledge of the mean normalized size. This essentially reduces the number of distribution function numerical parameters from 4 to 2.

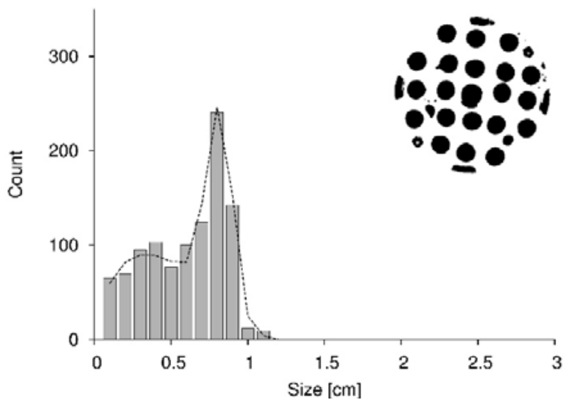

(a) Slightly damaged

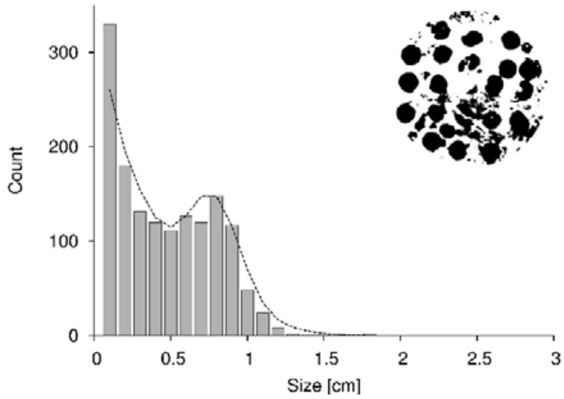

(b) Moderately damaged

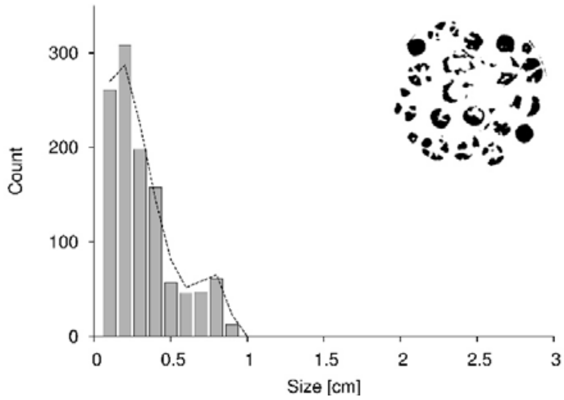

(c) Severely damaged

Figure 5 Example of the size distributions (vertical bars) at different stages of degradations and the approximate distribution functions (dotted lines).

6. CONCLUSIONS

A method to statistically characterize the porous structure of a severely damaged nuclear reactor core was developed in order to better analyze the evolution of damaged rods geometry.The particle and void size distributions are acquired for each tomography and then fitted with beta distribution functions so that each distribution can be characterized by the mean value and 2 shape parameters. The newly obtained distribution functions can then be used directly, as a representation of the porous structure, in appropriate applications such as in simulation codes or correlate the shape parameters of the functions with related properties of the media for further analysis.

Since the proposed method has been applied on variety of porous structures of the entire length of degraded fuel bundles with good results, it is expected that this method can also be applied to various types of porous structure in other applications, such as those in material and soil microstructure studies, which may have different distribution shapes. For instant, other distributions may show more than 2 distinct peaks, in which they need to be divided into several parts, but the procedure provided in Section 4 should remain applicable.

7. ACKNOWLEDGMENTS

The tomography data used in this study was kindly provided by the PHEBUS team at IRSN-Cadarache. We gratefully thank for their helps and supports.

REFERENCES

[1] Anderson, M.H., Oakley, J.G., Meekunnasombat, P. and Bonazza, R. **2005**. The Dynamics of a Shock Wave and Aluminum Foam Layer Interaction, *Proceedings of 25th International Symposium on Shock Wave (ISSW 25)*, Bangalore, India

[2] Fichot, F. *et al.* **2005**. The Use of a Diffuse Interface Model to Estimate Effective Transport Properties for Two-phase Flows in Porous Media, *Proceedings of 11th International Topical Meeting on Nuclear Thermal-Hydraulics (NURETH 11)*, Avignon, France.

[3] Ortega-Bernardo, M. and Fichot, F. **2000**. Post-test calculations of FPT1 test using ICARE2 V3MOD0 code: an alternative scenario, *Proceedings of 8th International Conference on Nuclear Engineering (ICONE 8)*, Baltimore MD, USA.

[4] Meekunnasombat, P., Fichot, F. and Quintard, M. **2006**. Numerical Simulation of Two-phase Flow in Severely Damaged Core Geometries, *Proceedings of 14th International Conference on Nuclear Engineering (ICONE 14)*, Miami FL, USA.

[5] Jacquemain, D., Bourdon, S., De Bremaechker, A. and Barrachin, M. **2000**. *PHEBUS PF FPT1-Final Report*, Document PHEBUS PF IP/00/479, IPSN/DRS/SEA/PEPF.

[6] WWW. http://www.xycoon.com/beta.htm (accessed on August 2005)